CHAPTER II

THEORETICAL STUDIES AND LITERATURE REVIEW

2.1 H_2 Permeation through a palladium membrane

The hydrogen permeation through a Pd membrane is a multi-step process [4, 5]. Figure 2.1 illustrates the different steps of the hydrogen permeation through the Pd membrane. Hydrogen molecules in the gas phase are adsorbed on the membrane surface, where they dissociate into hydrogen atom. The hydrogen atom diffuses through the Pd bulk, emerge at the permeate side of the membrane, and then reassociate back to form hydrogen molecule at the surface of the membrane, completing the permeation process. Each step of the hydrogen permeation through the palladium membrane is described in detail:

a. For the reversible dissociative chemisorption of hydrogen on the membrane surface $H_2 + 2\sigma \leftrightarrow 2H\sigma$, the flux can be expressed as the difference between desorption and adsorption rates (the adsorption rate is proportional to the H_2 pressure and the square of the vacancy (σ) on the membrane surface while the desorption rate is proportional to the square of the hydrogen coverage on the palladium surface)

$$J = -k_a P_{H_2} (1-\theta)^2 + k_d \theta^2 \qquad 2.1$$

Where θ is the surface hydrogen coverage, k_a and k_d are rate constants of the adsorption and desorption steps.

b. For the reversible dissolution of the surface atomic hydrogen in the dissolution interface of the palladium membrane, the flux is:

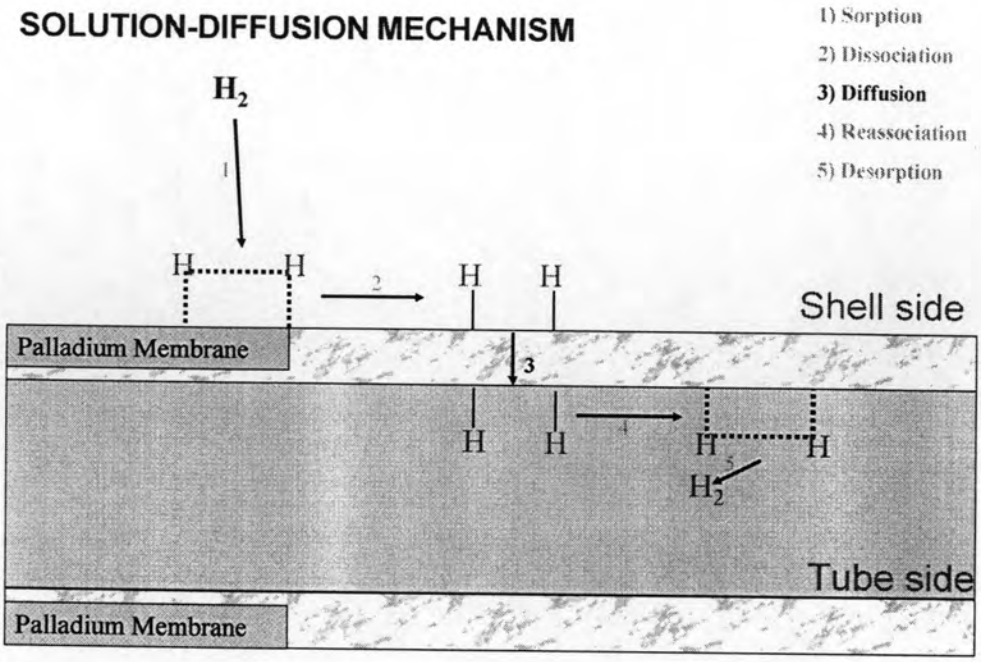

Figure 2.1 Illustration of the hydrogen permeation through Pd metal.

$$J = -k_O n\,(1-\theta) + k_i(1-n)\theta \qquad 2.2$$

Where k_o and k_i are rate constants of the dissolution and its reversed step and n is the atomic H/Pd ratio.

c. For the diffusion of the atomic hydrogen in the bulk of the membrane, the flux is:

$$J = \frac{D}{L}(C_{H_1} - C_{H_2}) \qquad 2.3$$

Where L is the thickness of the Pd membrane, D is the diffusivity of hydrogen in the palladium membrane; C_{H1} and C_{H2} are the hydrogen concentrations in the membrane immediately adjacent to the surfaces of the two sides. This can be conveniently expressed as:

$$C = K \cdot n \qquad 2.4$$

Where K is hydrogen concentration constant.

The step one and two take place on both faces of the membrane. These steps are fast; therefore the diffusion step is the rate-limiting step. The net flux for equations 2.1 and 2.2 is zero because the forward and reverse reaction rates are equal at equilibrium.

$$\frac{\theta}{1-\theta} = \left(\frac{k_a \cdot P_{H_2}}{k_d}\right)^{0.5} \tag{2.5}$$

$$\frac{\theta}{1-\theta} = \frac{k_o \cdot n}{k_i \cdot (1-n)} \tag{2.6}$$

Under the assumption of n<<1, the ideal behavior of a dilute solution and the rate limiting step being the hydrogen diffusion in the Pd bulk, the combination of Equations 2.5 and 2.6 gives Equation 2.7

$$P_{H_2}^{0.5} = \frac{k_o}{k_i}\left(\frac{k_d}{k_a}\right)^{0.5} n \tag{2.7}$$

or

$$n = \frac{k_i}{k_o}\left(\frac{k_a}{k_d}\right)^{0.5} P_{H_2}^{0.5} \tag{2.8}$$

Substitution of Equations 2.4 and 2.8 into 2.3 gives

$$J = \frac{DK}{L}\frac{k_i}{k_o}\left(\frac{k_a}{k_d}\right)^{0.5}\left(P_{H_2 h}^{0.5} - P_{H_2 l}^{0.5}\right) \tag{2.9}$$

or

$$J = \frac{DK}{Lk_s}\left(P_{H_2 h}^{0.5} - P_{H_2 l}^{0.5}\right) \tag{2.10}$$

$$k_s = \frac{k_o}{k_i}\left(\frac{k_d}{k_a}\right)^{0.5} \tag{2.11}$$

Where subscript h and l represent the hydrogen pressures at the high and low pressure sides, respectively.

Since D and k_s have and exponential relation with temperature and K is a constant, the term of $\frac{DK}{k_s}$ can be written as: $Q_o \cdot exp\ (\frac{-E_P}{RT})$

$$\frac{DK}{k_s} = Q_o \cdot exp\ (\frac{-E_P}{RT}) \qquad 2.12$$

Where Q_o and E_p are the permeability coefficient and permeation activation energy respectively. Therefore, Equations 2.10 becomes

$$J = \frac{Q_o}{L} \cdot exp\ (\frac{-E_P}{RT}) \cdot (P_{H_2h}^{0.5} - P_{H_2l}^{0.5}) \qquad 2.13$$

Equation 2.13 is the so-called Sievert's law. The H_2 permeation flux is inversely proportional to the thickness of the Pd layer and directly proportional to the difference of the square roots of the hydrogen pressures.

The Sievert's law can also be obtained in the simplified way. The dissolution of hydrogen in the palladium can be expressed as:

$$\frac{1}{2} H_2 = H_{(abs)} \qquad 2.14$$

The equilibrium equation can be written as:

$$P_{H_2}^{0.5} = kC_H \qquad 2.15$$

Substitution of Equation 2.15 into Equation 2.3 gives

$$J = \frac{D}{LK} \cdot (P_{H_2h}^{0.5} - P_{H_2l}^{0.5}) \qquad 2.16$$

$$J = \frac{Q}{L} \cdot (P_{H_2h}^{0.5} - P_{H_2l}^{0.5}) \qquad 2.17$$

Where $Q = \frac{D}{K} = Q_o \cdot exp\ (\frac{-E_P}{RT})$

Equation 2.17 can be also written as:

$$J = \frac{Q_o}{L} \cdot exp\left(\frac{-E_P}{RT}\right) \cdot \left(P_{H_2h}^{0.5} - P_{H_2l}^{0.5}\right) \qquad 2.18$$

2.2 Dry reforming reaction

The thermodynamics of the carbon dioxide reforming with methane has been deeply investigated [3]. The corresponding carbon dioxide reforming reaction is described as

$$CH_4 + CO_2 \rightarrow 2CO + 2H_2 \qquad \Delta H_{298}^o = 247\ kJ/mol \qquad 2.19$$

$$\Delta G^o = 61770 - 63.32T\ kcal/mol$$

This reaction is highly endothermic and is equally favored by low pressure but requires a higher temperature. A reverse water-gas shift reaction occurs as a side reaction:

$$CO_2 + H_2 \rightarrow CO + H_2O \qquad \Delta H_{298}^o = 41\ kJ/mol \qquad 2.20$$

$$\Delta G^o = -8545 + 7.84T\ kcal/mol$$

Under conditions of stoichiometric CO_2 reforming, carbon deposition occurs as in the Boudouard reaction [6].

$$2CO_2 \rightarrow C + CO_2 \qquad \Delta H_{298}^o = -171\ kJ/mol \qquad 2.21$$

$$\Delta G^o = -39810 - 40.87T\ kcal/mol$$

And in the methane cracking

$$CH_4 \rightarrow C + 2H_2 \qquad \Delta H_{298}^o = 75\ kJ/mol \qquad 2.22$$

$$\Delta G^o = -21960 - 26.45T\ kcal/mol$$

The standard free energy change was employed to calculate the minimum operation temperatures for CO_2 reforming and CH_4 cracking, and the upper limiting temperatures of the other side reactions (2.20) and (2.21). Assuming $\Delta G° = 0$, the upper or lower limiting temperatures for reactions (2.19)-(2.22) will be obtained. CO_2/CH_4 reaction can proceed above 645°C accompanied by methane cracking reaction, while above 817°C reverse water gas shift reaction and the Boudouard

reaction could not occur. In the temperature range of 557~700°C carbon will be formed from methane cracking of the Boudouard reaction.

Table 2.1 Limiting temperatures for reactions in the CO_2/CH_4 system

	Reaction			
	1[a]	**2[b]**	**3[b]**	**4[a]**
Temperature /°C	645	817	700	557
Reaction type	Reforming	RWGS	CO→CO	CH_4 cracking
Reaction taking place	≥645	≤817	≤700	>557

a: Lower limit and b: Upper limit

Nowadays, two viewpoints have been proposed about the mechanism of carbon dioxide reforming with methane, the general opinion is firstly; methane is adsorbed, activated and dissociated on the reduced metal catalyst. Nevertheless, the divaricating occurs about whether carbon dioxide also dissociate on the surface of the catalyst. Takayasu and Matsuura [7] suggested that gaseous carbon dioxide directly reacts with hydrogen formed from methane to water, steam reforming then followed to obtain synthesis gas. That is to say, the substance of the carbon dioxide reforming is the same as the steam reforming.

Erdohelyi *et al.* [8] reported the studies of the decomposition of methane on the supported Rh catalyst employing temperature-programmed reduction and pulse reaction technique. The results indicated that methane might decompose even at 150°C. The *in-situ* infared spectra studies indicated that pure carbon dioxide might dissociate on Rh/Al_2O_3 catalyst above 250°C.

The reaction of methyl species on Ni (111) and Ni (100) was studied employing mass spectroscopy [9]. The results showed that the C-H rupture of methyl readily occurs at -53.15°C. It gave good evidence that C-H rupture of fairly stable methyl is easy. As mentioned above, the activation of methane on VIII group metals is not very difficult. The strong chemisorption of CH_x and hydrogen formed by methane on metals may large decrease the energy barrier of dehydrogenation of

methane and promotes the stepwise dissociation at lower temperature. Compared with VIII group metals, the metal oxide catalysts do not have the strong interaction with methane and CH_x. So, the very high temperature is necessary for the activation of methane to supply enough energy.

Erdohelyi *et al.* [8] proposed the mechanism of carbon dioxide reforming with methane over supported noble metal catalysts on the basis of kinetic studies. Methane may undergo two reactions as following routes: stepwise dehydrogenation followed by the surface reaction with surface oxygen or OH to CO and H_2 (1) or direct reaction with surface oxygen species to CH_x then follow former route (2) carbon dioxide may react with adsorbed hydrogen, surface carbon and surface CH_x fragments.

The proposed mechanism is as follows:

$$CH_4 \xrightarrow{M} CH_{x(ad)} + H_{(ad)} \ (x = 0 \approx 3)$$

$$CH_4 + O_{(ad)} \xrightarrow{M} CH_{3(ad)} + OH_{(ad)}$$

$$CO_2 + H_{(ad)} \xrightarrow{M} CO + OH_{(ad)}$$

$$2OH_{(ad)} \xrightarrow{M} H_2O + O_{(ad)}$$

$$CH_{x(ad)} + O_{(ad)} \xrightarrow{M} CO + xH_{(ad)}$$

$$CH_{x(ad)} + CO_2 \xrightarrow{M} 2CO + xH_{(ad)}$$

$$2H_{(ad)} \xrightarrow{M} H_{2(g)}$$

$$C_{(ad)} + CO_2 \xleftrightarrow{M} 2CO$$

$$C_{(ad)} + H_2O \xrightarrow{M} CO + H_2$$

The mechanism of carbon dioxide reforming with methane may somewhat change when different types of catalysts are used. Zhang *et al.* [10] reported that Ni/La_2O_3 catalyst showed high stability because a new reaction pathway occurred at the Ni/La_2O_3 interface. They proposed a mechanism that under the CO_2/CH_4 reaction conditions, CH_4 mainly cracks on the Ni crystallites to form H_2 and surface carbon species (CH_x species), while CO_2 is preferably adsorbed on the La_2O_3, support or the LaO_x species which are decorating the Ni crystallites in the form of $La_2O_2CO_3$. At high temperatures the oxygen species of $La_2O_2CO_3$ may participate in reactions

with the surface carbon species (CH_x) on the neighboring Ni sites to form CO. Owing to the existence of such synergetic sites which consist of Ni and La elements, the carbon species formed on the Ni sites are favorably removed by the oxygen species originated from $La_2O_2CO_3$, thus resulting in an active and stable performance.

The temperature-programmed oxidation experiments have been conducted employing isotope labeled $^{13}CH_4$ over Rh/Al_2O_3 catalyst in the carbon dioxide reforming system [10]. The results showed that carbon deposition on the catalyst primarily derived from carbon dioxide and lesser extent from methane. The reported mechanism of carbon dioxide reforming cannot explain this fact reasonably. The further studies are necessary for elucidation the detailed reaction pathway and mechanism.

Yan *et al.* [11] reported that the decomposition of methane on nickel catalyst could result in the formation of at least three kinds of surface carbon species on supported nickel catalyst. Generally, the carbon deposition comprises various forms of carbon which are different in terms of reactivity. The distribution and features of these carbonaceous species depend sensitively on the nature of transition metals and the conditions of methane adsorption. These carbonaceous species can be described as: completely dehydrogenated carbidic C_α type, partially dehydrogenated CH_x ($1 \leq x \leq 3$) species, namely C_β type, and carbidic clusters C_γ type formed by the agglomeration and conversion of C_α and C_β species under certain conditions. A fraction of the surface carbon species, which might be assigned to carbidic C_α (~187.85°C), was mainly hydrogenated to methane even below 226.85°C. It showed the carbidic C_α species was suggested to be responsible for CO formation. A significant amount of surface carbon species were hydrogenated to methane below 326.85°C and were assigned to partially dehydrogenated C_β (~309.85°C) species. The majority of the surface carbon was hydrogenated above 526.85°C and was attributed to carbidic cluster C_γ (~549.85°C). The possible reaction processes of carbon dioxide reforming with methane was inferred as follows: methane is firstly decomposed into hydrogen and different surface carbon species, then the adsorbed CO_2 reacts with surface carbons to form CO.

The proposed mechanism is as follows [11].

1) Dissociative adsorption of methane is the rate-determining step.

$$CH_{4\,(g)} \rightleftharpoons CH_{4\,(ad)} \rightleftharpoons CH_{x\,(ad)} \rightleftharpoons (4\text{-}x)H_{(ad)} \rightleftharpoons Carbon_{(ad)} + xH_{(ad)}$$

2) Dissociative adsorption of carbon dioxide.

$$CO_{2\,(g)} \rightleftharpoons CO_{2\,(ad)} \rightleftharpoons CO_{(ad)} + O_{(ad)} \rightleftharpoons Carbon_{(ad)} + O_{(ad)}$$

3) Formation of water.

$$2H_{(ad)} + O_{(ad)} \rightleftharpoons H_2O_{(ad)} \rightleftharpoons H_2O_{(g)}$$

4) Formation of hydrogen.

$$2H_{(ad)} \rightleftharpoons H_{2(ad)} \rightleftharpoons H_{2(g)}$$

5) Formation of carbon monoxide and decarbonation.

$$CO_{(ad)} \rightleftharpoons CO_{(g)}$$

$$Carbon_{(ad)} + O_{(ad)} \rightleftharpoons CO_{(ad)} \rightleftharpoons CO_{(g)}$$

This mechanism is actually the synergic decomposition process of methane and carbon dioxide Scheme 2.1

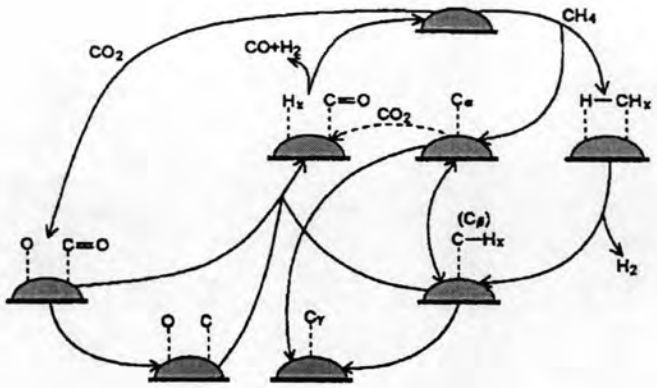

Scheme 2.1 Patterns of activation and reaction of methane with carbon dioxide on the metal catalyst.

2.3 Literature Review

2.3.1 H_2 Permeable membrane

2.3.1.1 Oxide membrane

One of the H_2 permeable membranes is an oxide membrane. The studies of H_2 permeable oxide membranes concentrated mainly on deposition of an oxide layer, such as silica or titania onto the porous membrane supports. The precursor agents included several types of silicon compounds, such as SiH_4, $SiCl_4$ and $(C_3H_7)_3SiH$ was used for preparing the dense silicate layer on the top of the Vycor glass. The reported separation ratio for H_2/N_2 ranged from hundred to 2,000, depending on the temperatures (from 450°C to 750°C). The reported H_2 permeances, however, were extremely low, ranging from only 0.33 to 0.0012 m^3 (STP)/ (m^2·h·atm), partially limited by the permeance of initial Vycor glass supports, *ie.* ~0.38 m^3 (STP)/(m^2·h·atm). They proposed solid-phase diffusion as a possible transport mechanism. Hydrogen molecules dissolved in and then diffused through the silicate film, thus delivering an extremely high selectivity. The observed N_2 flow might be caused by Knudsen diffusion through a few cracks or large pores.

Most of these Hydrogen-selectivity membranes demonstrated an impressive H_2 selectivity (*i.e.*, several hundreds to thousands), but suffered from a common

problem: the H_2 permeance was too low to be economically feasible for industrial applications, such as H_2 separations or catalytic membrane reactors. Since the permeance is normally enhanced through the sacrifice of the selectivity, balanced permeance and selectivity are essential to achieve optimum performance.

2.3.1.2 Palladium membrane

Pd membranes have been extensively studied because of their exceptional hydrogen-separating capabilities. Hydrogen permeation through a Pd-based membrane is a complex process Athayde *et al.* [5] including hydrogen chemisorption, dissolution into the Pd lattice, diffusion in the bulk of the Pd layer driven by the concentration gradient and, finally, desorption from the opposite surface. In most cases, the hydrogen diffusion in the bulk of the Pd layer is believed to be the rate-controlling step Shu *et al.* [12]. The H_2 permeance through the Pd layer follows the Sievert's law, which reveals that the H_2 permeance is proportional to the difference of the square roots of hydrogen pressures and inversely proportional to the thickness of the Pd membrane.

The H_2 permeance flux has not always been found to vary linearly with the difference of the square roots of hydrogen partial pressure. The Sievert's law described the pressure dependency of hydrogen permeation as exponent through the palladium membrane under the ideal situation such as dilute solution behavior and no contamination on the surface of the membrane. In reality, the powers of the hydrogen partial pressure might be greater than 0.5 due to some reasons like deviation from dilute solution behavior, non-steady state operation, different rate-limiting step and surface contamination.

In recent years, deviations from Sievert's law have been further reported with composite thin Pd membranes. Uemiya *et al.* [13] determined a 0.76 power dependence on pressure using a Pd/porous glass membrane prepared by the electroless plating, with a Pd thickness of 20 μm, and attributed the higher power dependence to a dependence of diffusivity on the changes in hydrogen concentration in the membrane. In addition, Collins and Way [14] have obtained power dependence varying from 0.52 to 0.73, also with electroless-plated composite Pd membrane with thickness between 11.4 and of 20 μm. Interestingly, it was observed that the thinner

the Pd membrane, the higher the power dependence, indicating the change of the rate-controlling step from the diffusion of hydrogen in the bulk of the bulk of the Pd membrane to the surface process.

The rate-limiting step of the H_2 permeation can also be influenced by temperatures. Chabot *et al.* [15] pointed out that at temperature below 200°C, the sorption and dissociation steps at metal surfaces appeared to be the rate-controlling step, and the hydrogen flux was no longer inversely proportional to the membrane thickness. At temperatures lower than 300°C, the surface sorption and dissociation process tended to be slow, and the rate-controlling step seemed to shift to surface process. This was supported by the data of Holleck [16]. Thus, the power of the pressure was greater than 0.5.

The permeation of gases other than hydrogen through thin palladium membrane was frequently observed. Theoretically, a palladium membrane should have infinite selectivity for hydrogen. However, since the palladium membrane is typically a polycrystalline film with a fine grain structure, the grain boundaries [5] can form pathways for the diffusion of other gases, which limit the attainable infinite selectivity.

Bryden and Ying [17] reported that the hydrogen diffusion coefficient through a single-crystalline palladium can be improved by making nanostructure palladium or its alloys because compared to bulk palladium, the grain boundary has such as a large volume that hydrogen can rapidly diffuse. Namely, a polycrystalline palladium membrane with small grain can show superior hydrogen permeability.

2.3.2 Preparation of palladium membranes

2.3.2.1 Electroless plating

The principle of the electroless plating technique is based upon the controlled autocatalyzed decomposition or reduction of metastable metallic salt complexes on target surface [12, 18]. Thus, this technique can also be applied to the formation of

metal coating even on a non-conductive support such as porous ceramic and glass since no current is needed.

Palladium composite membranes were successfully prepared with electroless plating technique by several investigators [18]. Table 2.1 lists some examples of the Pd membranes prepared by the electroless plating. As shown in Table 2.1, the Pd or its alloy membranes were deposited on the porous glass [19, 20, and 21], the porous alumina tubes [14, 22], porous ceramic disk [23], porous silver disks [24], and porous stainless steel supports [25, 26, and 27]. The prepared membranes exhibited good hydrogen permeation, but the data on long term stability were scarce.

Table 2.2 Examples of the Pd membranes prepared by electroless plating

Metal	Support	Main Results	Ref.
Pd	Glass tube o.d. 10 mm 0.8 mm thickness	13 μm Pd thickness H_2 Permeation flux 7.62 $m^3/(m^2 \cdot atm \cdot h)$ at 500°C Apparent activity energy 10.7 kJ/mol	[19]
Pd	Alumina tube Pore size 10-200 nm	11.4 μm Pd thickness Pd:H_2 Permeability 23.6 $m^3/(m^2 \cdot atm^{0.602} \cdot h)$ H_2/N_2 selectivity 380 at 549.85 °C and 14.804 atm	[14]
Pd-Ag	316L stainless steel Disk 0.5 μm pore size	The codeposition of Pd and Ag is passivated by the preferential deposition of Ag. No H_2 peameation of the Pd-Ag alloy membrane was given.	[25]
Pd	316L stainless steel tube	19-28 μm Pd thickness Pd:H_2 Permeability 2-4 $m^3/(m^2 \cdot atm \cdot h)$ H_2/N_2 selectivity 3000 at 350°C and 1 atm	[27]
Pd-Ag	Glass tube	No information about thickness H_2 Permeation flux 0.84 $m^3/(cm^2 \cdot atm \cdot h)$ H_2/He selectivity 3.0 at 499.85°C	[21]
Pd	316L stainless steel tube	10 μm Pd thickness H_2 Permeation flux 3.9 $m^3/(m^2 \cdot atm \cdot h)$ H_2/N_2 selectivity 850 at 427°C and 1.344 atm	[26]
Pd	Alumina tube	11-17 μm Pd thickness H_2 Permeation flux 20.2 $m^3/(m^2 \cdot atm \cdot h)$ H_2/N_2 50 at 773 K and 6.805 atm	[22]

The Pd salt widely used in the plating was $[Pd(NH_3)_4]Cl_2$ or $[Pd(NH_3)_4](NO_3)_2$. The reducing agent used early was sodium hypophosphite that could result in the deposition of phosphorous impurity on the membrane. Auger spectrometry showed that the Pd layer produced by using hypophosphite contained about 5% phosphorous impurity. Currently, hydrazine has been widely applied as the reducing agent instead of sodium hypophosphite since hydrazine does not yield any contaminants in the Pd deposition. Disodium ethylenediaminetetraacetate (EDTA) was used as a stabilizer.

Shu *et al.* [25] studied the co-deposition behavior of palladium and silver on a porous stainless steel disk by the electroless plating. It was found that the simultaneous deposition was passivated by the preferential deposition of silver. An improved co-deposition was achieved by the Pd predeposition. A combination of XRD and EDS analysis revealed that the co-deposited Pd and Ag were in separate phases and that small amounts of an amorphous palladium rich phase were also present in the deposited material. Thermal treatment of co-deposited Pd-Ag films in H_2 atmosphere created Pd-Ag alloy membranes on the porous stainless steel substrate. The key point in the co-deposition of Pd-Ag for a specific ratio of Pd/Ag was to balance the deposition rate of individual species by adjusting the concentration of the stabilizer and metals salts.

In order to improve the electroless plating technique, Yeung and Varma [28] attempted the preparation of the thin metal-ceramic composite membranes by modifying conventional electroless plating with the use of osmosis. They reported that; the osmosis pressure was used to densify an existing supported metal membrane, the densification and growth of the film was managed under the influence of osmotic pressure by using a dilute plating solution, and films of varying porosity were deposited on the ceramic membrane by combining electroless deposition and osmotic pressure.

Yeung and Varma [28] examined the thermal stability of the thin films prepared with and without osmotic pressure by using the SEM analysis. The films were subjected to heat treatment under oxygen at 350°C for 55 hours, and the resulting microstructures were imaged using SEM. It was reported that the silver, palladium, and palladium-silver films prepared with osmotic pressure on alumina membranes were thermally more stable than the similar films deposited by the conventional electroless plating. However, the authors did not report any hydrogen permeation and separation data.

The presence of tin originated from the activation step with stannous chloride solution and palladium chloride solution was believed to relate to the reduction of hydrogen permeation at high temperatures. Improved activation procedure without tin was attempted recently. Li *et al.* [26] used a sol-gel technique in which palladium salt

modified boechmith sol was deposited on the surface of the porous alumina, followed by calcinations at 550°C and hydrogen reduction at 400°C. They reported that the Pd deposition rate on the support activated by the improved procedure was faster than that by the conventional activation procedure (the $SnCl_2$ and $PdCl_2$ activation procedure). However, no H_2 permeation was given. Recently, Paglieri *et al.*[22] proposed a new tin-free procedure. Prior to electroless-plating, substrates were dip-coat in a chloroform solution of Pd acetate, dried calcined, and then reduced in flowing hydrogen. The resulting supported membrane prepared using this new procedure exhibited a constant hydrogen flux at 550°C for a period of one week. However, the H_2 permeation decreased at 550°C and above because of annealing.

2.3.2.2 Sputtering

This technique involves bombarding a target with energetic particles that cause surface atoms to be ejected and then deposited on a substrate close to the target [12]. Its configuration of such instrument is exhibited as Figure 2.2.

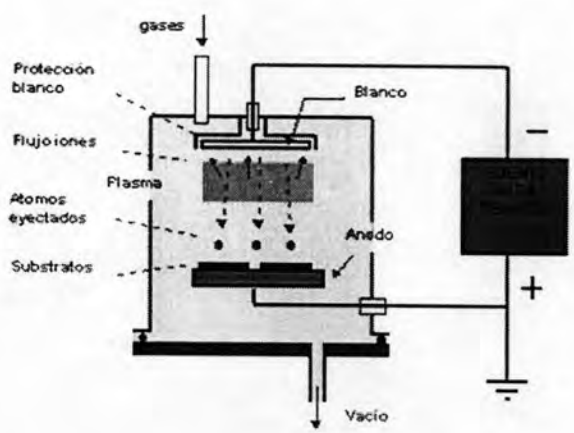

Figure 2.2 Sputtering instrument.

The main advantage of this particular technique is that the evaporation rate is quite similar from one metal to another and therefore the technique is most suitable for the deposition of alloys. On the other hand, it is difficult to deposit a thin film using sputtering on certain supports such as a tube used widely in industries. Also, sputtering could not be used for coating the inside tube surface.

Gryaznov *et al.*[29] prepared thin films of binary and ternary alloys of palladium with manganese, cobalt, ruthenium, tin and lead on symmetric polymeric membranes, porous stainless steel sheets and oxide supports by the sputtering technique. The membranes prepared by Gryaznov were only permeable to H_2 and stable at 200°C The hydrogen permeance was 13.8 $m^3(STP)/(m^2h)$ at 200°C and 1 MPa.

Jayaraman and Lin [30] deposited ultrathin palladium-silver layer on a porous α-alumina disk by an RF magnetron sputtering equipment. The Pd-Ag membrane with a thickness in the range of 250-500 nm exhibited the hydrogen to nitrogen separation factor to be 5.7 at 250°C. Such a low separation factor implied that the membranes were not dense and might have pinholes.

Bryden and Ying [17] also prepared the nanostructured palladium on the porous Vycor glass by magnetron sputtering. Heating the ultrathin nanostructured palladium membranes to 200°C led to some grain growth. The stabilization against the phase transition and grain coarsening was critical to applications for nanostructured membranes in hydrogen separations, and could be achieved by alloying palladium with another metal.

2.3.2.3 Chemical vapor deposition (CVD)

In the CVD process, a chemical reaction involving a metal complex in the gas phase is carried out at a controlled temperature. The metal produced by this reaction deposited as a thin film by nucleation and growth on the substrate. The instrument is showed in Figure 2.3.

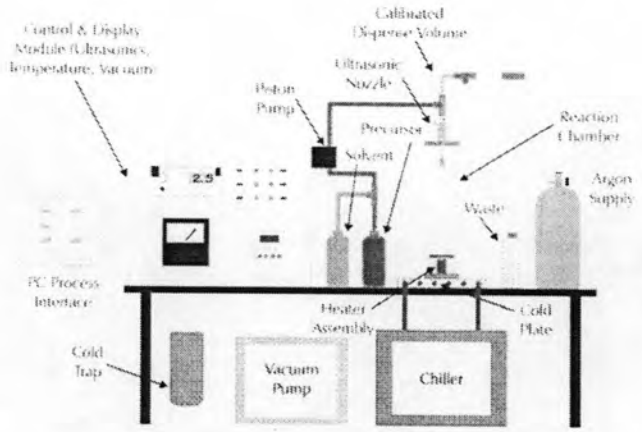

Figure 2.3 Chemical vaporization deposition.

The CVD technique was widely used to deposit an oxide layer on a support or to block holes in the support. Yan *et al.*[31] attempted to prepare a palladium membrane inside the porous wall of an α-alumina tube by the metal-organic chemical vapor deposition (MOCVD). For the membrane prepared with a maximum CVD temperature of 300°C, the hydrogen permeance and the selectivity to nitrogen in the range of 300-500°C were respectively higher than $8.1 m^3(STP)/(m^2h)$ and 1000 when the hydrogen pressure in the upstream side was about 0.1 MPa. The authors reported the resistance to hydrogen embrittlement but no explanation was given.

2.3.3 H_2 Embrittlement in palladium membranes

The H_2 embrittlement was a severe problem for the application of a palladium membrane for hydrogen separation. Pd-hydrogen interactions gave rise to a β-phase below about 300°C and α-phase above 300°C in Figure 2.4

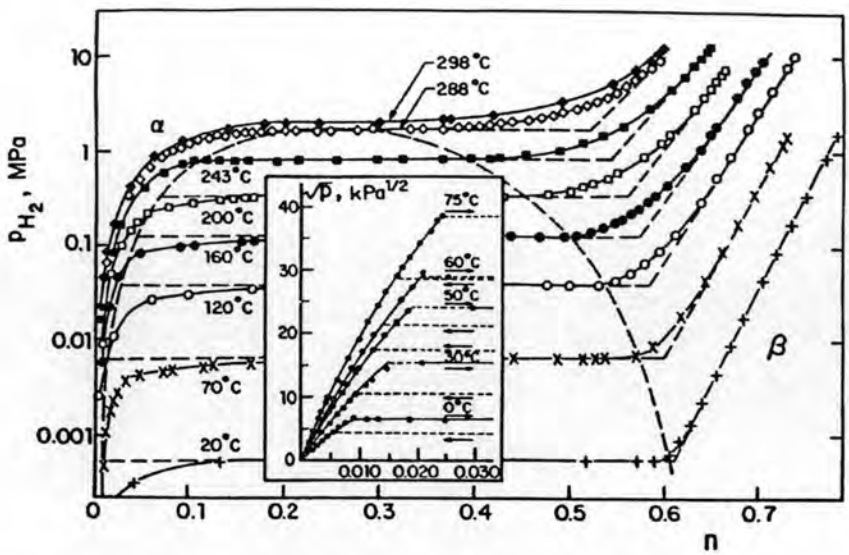

Figure 2.4 Equilibrium isotherms of Pd-H system (n=H/Pd) [12].

The α-β-transformation caused serious alteration in the atom spacing of the metal lattice. The resulting dimensional changes were large enough to distort the membrane, marking it less mechanically resistant, and more brittle and prone to rupture, i.e., so called H_2 Embrittlement. Shu *et al.*[12] also reported the H_2 Embrittlement that as soon as the temperature was below 300°C and the pressure below 2.0 MPa, the β-hydride nucleated from the α-phase which resulted in severe lattice strain. It will create the crack on the membrane surface exhibited as Figure 2.5.

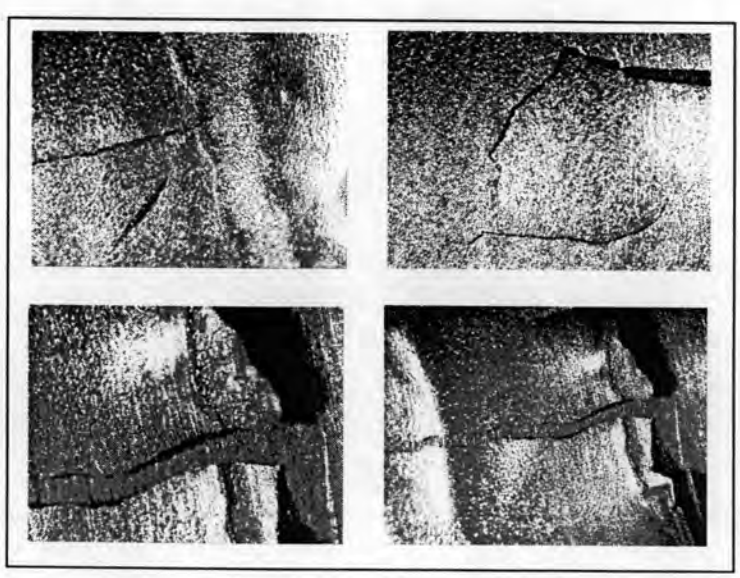

Figure 2.5 The crack taking place on the membrane surface because of the H_2 embrittlement.

Therefore, 300°C was the minimum preferred operating temperature for pure Pd membranes. In their experiments, Uemiya *et al.* [18] noted that the Pd layer coated on the ceramic support developed pin-hole cracks when exposed to hydrogen at less than 300°C due, probably, to the α-β-transformation in the palladium membranes.

One way to overcome the H_2 embrittlement was to alloy palladium with some other metals. It was reported that the hydrogen embrittlement temperature could be brought down to 200°C by adding copper or silver into palladium [33, 34]. Alloying Pd with Ru, Rh, and other metals has been found to suppress the α→β phase transition even at the room temperature [1]. This could be explained by an increase in the interstitial spacing of the metal matrix.

Al-Shammary *et al.* [36] reported that by alloying palladium with 10% yttrium, the permeability was enhanced by nearly 4 times. Extensive research on the transport rate dependence on the Pd alloy composition has shown that the 25% Ag/75% Pd alloy yielded the highest solubility of H_2 (about 0.001 g/g at 300°C and 0.0003 g/g at 500°C) with the highest flux [37]. The equilibrium sorption of hydrogen in the palladium/silver alloy increase as the relative amount of silver in the alloy increased. However, the diffusion coefficient of hydrogen in the alloy decreased with increasing silver content. As a result of these two opposing trends, the hydrogen permeability for a palladium/silver alloy had its maximum value at a silver content of 23-25 atom%.

2.3.4 Intermetallic diffusion of palladium metal membranes

The intermetallic diffusion has recently received increasing attention for composite Pd metal membranes since H_2 permeation flux declined rapidly when the intermetallic diffusion occurred [38, 39]). Edlund and Pledger [40] constructed the composite Pd-V-Pt metal membrane with the intermediate layers of SiO_2 as a barrier to the intermetallic diffusion. As the membrane reactor for the thermolysis of H_2S, the composite membrane showed no change in the H_2 permeation for 8 hours at 700°C and 7.8 bar pressure. The author claimed that this membrane maintained a good thermal stability.

More recently, Gryaznov *et al.*[29] also encountered the intermetallic diffusion in their Pd-Ru/porous stainless steel disc membranes. The hydrogen permeation declined twofold at 800°C after 1000 hours. The XPS spectra revealed the diffusion of steel components to the outer surface of the palladium alloy film. An intermediate layer like alumina, magnesia, zirconia, or tungsten was used as a barrier to the intermetallic diffusion. The layer thickness ranged from 0.8 to 1.2 μm and the results showed no decreasing trend in the hydrogen permeation. However, the author did not mention in detail how to insert this intermediate layer.

2.3.5. Membrane reactors

2.3.5.1 Short history of membrane reactors development

The first membrane reactors used palladium alloys as membrane. The unique property of palladium to absorb great amounts of hydroxyl was discovered by T. Graham in 1861. He was the first who used a Pd tube as a membrane with selective permeability for H_2. Much later M. Temkin and colleagues applied a Pd tube membrane for diffusion supply of H_2 to ethylene in their study of the ethylene hydrogenation mechanism.

However the concept of "membrane catalysis" was formulated only in the 1960s by V.M. Gryaznov [42].

Table 2.3 Summaries of the basic milestones in the history of metal-containing membranes and reactors in the twentieth century

Year	Event	Country
1861	Graham discovered the selective permeability of Pd for H_2 and hydrogenating ability of H_2 dissolved in Pd.	UK
1958	Temkin and Apellbaum used Pd membranes for the study of mechanism of ethylene hydrogenation.	USSR
1964	Grgaznov Smirnov Mischenko, and Ivanova discovered reaction coupling on Pd membrane catalysts.	USSR
1964	Pfefferle carried out the coupling of ethane dehydrogenate and hydrogen oxidation by O_2 a Pd membrane.	USA
1966-1969	Wood and Wise used a Pd-Ag tube membrane for the study of cyclohexane dehydrogenation and benzene hydrogenation.	USA
1969	Gryaznov and Gulianova carried out ethylene oxidation and silver tube as membrane catalyst.	USSR
1970	The elaboration by Gryaznov and colleagues of the variety of binary Pd alloys for hydrogenation and dehydrogenation of different compounds and creation of membrane reactor design.	USSR
1974	The starting of a pilot unit on toluene hydrodemethylation with a membrane reactor consisting of 196 Pd–Ni alloy tubes.	USSR
1979	The first composite palladium-polymer membrane catalyst was prepared by Grayznov, Vdovin et al. and used for cyclopentadiene hydrogenation.	USSR
1981	The first pilot unit for liquid-phase dehydrolinalool hydrogenation started with a membrane reactor contain flat spirals from Pd-Ru alloy.	USSR
1985	Otzuka et al. carried out methane coupling on Ag/YSZ membrane.	Japan

Year	Event	Country
1986	Suzuki carried out a number of hydrogenation and dehydrogenation reactor on zeolite membrane catalyst.	Japan
1990	Kikuchi and Uemiya used a composite palladium membrane on a porous support.	Japan
1991	Burgraff and Ross carried out methanol reforming on a catalytically activity ceramic membrane prepared by the sol-gel technique.	Netherlands
1994	Tokyo Gas Co., Ltd started the first pilot plant for methane steam reforming with a composite ceramic membrane reactor.	Japan
1997	Eltron Research Inc. started a plant for syngas production by ion-permeable membrane technology.	USA

2.3.5.2 Reactions in membrane reactors

Recently a number of equilibrium-limited reactions have been investigated using inorganic membrane (either nonporous or porous) reactors [43, 44, 45, 46, and 47]. The dense metal membranes are characterized by the high selectivity with a relatively low permeation flux compared to porous ceramic membranes. On the other hand, the porous ceramic membranes give high permeation rates, but low selectivity due to the fact that the permeation is primarily governed by Knudsen diffusion.

One class of the reactions studied widely in membrane reactors is the dehydrogenation of hydrocarbons. The dehydrogenation reactions are usually endothermic so that equilibrium constants increase with the increase in the temperature. At low temperatures the dehydrogenation conversion is thus often severely limited by the restriction of thermodynamic equilibrium. In such a case, the instantaneous removal of hydrogen in the reaction zone by the permeation through a membrane (either porous ceramic or palladium one) can in principle increase the conversion.

A number of papers have been recently published on the use of porous ceramic membranes for catalytic dehydrogenation reactions. Itoh *et al.* [48] studied the dehydrogenation of cyclohexane to benzene using a Vycor glass membrane reactor with a mean pore size of 40Å. The catalyst was placed in the bore of the membrane tube. The conversion at 200°C and 1atm pressure was 45% versus the 19% equilibrium value

Also, a great number of dehydrogenation reactions have been investigated in palladium or its alloy membrane reactors and good results in the conversion and selectivity were observed. Table 2.2 listed some examples of dehydrogenation reactions carried out in palladium membrane reactors.

Compared to porous membrane reactors, palladium membrane reactors give considerably high selectivity to hydrogen. The hydrogen produced in the reactors can be more selectively removed in the palladium membrane reactors. Therefore, the conversions in the palladium membrane reactors are higher than those in the porous membrane reactors. For example, the conversion in the reaction of cyclohexane to benzene in Table 2.2 was 99.7% in the Pd-Ag membrane reactor [49]. On the other hand, the conversion of the same reaction in the porous membrane reactor was only 45% as mentioned previously [48].

Also, as listed in Table 2.2, the conversions obtained in the palladium reactors were, in general, considerably higher than the equilibrium values. For example, Sheintuch and Dessau [50] studied the dehydrogenation of isobutene and propane in a palladium-based membrane reactor. Significant grains in yield were achieved in the membrane reactor: up to 76% butane yield at 500°C (32% at equilibrium) and 70% propene yield at 550°C (23% at equilibrium).

Table 2.4 Palladium membrane reactors for some dehydrogenation reactions

Reaction	Membranes	Main results	Ref.
$C_6H_{12} \rightarrow C_6H_6 + 3H_2$	Pd /Ag (23%) tube	Temperature 200°C C 99.7% C_{eq} 18.7%	[49]
$CO + H_2O \rightarrow CO_2 + H_2$	Pd /Vycor tube	Temperature 400°C C 99% C_{eq} 78%	[13]
$H_2S \rightarrow H_2 + S$	Pt-SiO_2-V-SiO_2-Pd disk	Temperature 700°C C 99.4% C_{eq} 13%	[39]
$C_4H_{10} \rightarrow C_4H_8 + H_2$ $C_3H_8 \rightarrow C_3H_6 + H_2$	Pd/Ag tube	For C_4H_{10} Temperature 500°C C 76%, C_{eq} 32% For C_3H_8 Temperature 550°C C 70%, C_{eq} 23%	[50]
$C_3H_8 \rightarrow C_3H_6 + H_2$	Pd/Al_2O_3 tube	Temperature 550°C C 70% Without membrane C 30%	[51]
$CH_4 + H_2O \rightarrow CO + 3H_2$	Pd/Al tube	Temperature 550°C C 45.7% Without membrane C 34.7%	[52]
$CH_3OH \rightarrow 2H_2 + CO$	$Pd_{91}Ru_6In_3$ tube	Temperature 220-250°C C 72% Without membrane C 48%	[53]

Remark: C: conversion C_{eq}: conversion at equilibrium

2.3.5.3 Dry reforming by using membrane reactor

There are a few research groups deal with membrane reactor for improving the methane conversion such as Galuszka *et al.*[52], Ferreira-Aparicio P. *et al.*[55, 56, 57], and Munera *et al.*[58].

Galuszka *et al.* [52] was the first group studying the application of palladium membrane supported on alumina by electroless plating. The dry reforming reaction was performed at 350°C to 600°C. It was found that CH_4 conversion increased between 4-20%. The CO and H_2 yield increased between 2-20% and 8-18%, respectively, when Pd/Al_2O_3 was used. However, the palladium membrane swelled due to the thermal expansion difference between palladium layer and alumina support.

Ferreira-Aparicio *et al.* [55, 56] found that the methane conversion was improved by using mesopore ceramic membrane. The reaction was performed at 550°C. It was found that the methane conversion was 16% whereas the carbon dioxide conversion was 25% when Pd/Al_2O_3 was used. Since mesopore ceramic membrane was a porous membrane the selectivity of membrane was very low.

Munera *et al.* [58] reported that dense Pd/Ag composite membrane can improve the methane conversion by using Rh/La_2O_3 and Pd/La_2O_3 as a catalyst in this study.

Ferreira-Aparicio *et al.* [57] studied palladium membrane supported on porous stainless steel. The reaction was performed at 510°C with Ni/Al_2O_3, Ni/ZrO_2, Ni/ZrO_2-CeO_2, and $Ni/Ce_{0.5}Zr_{0.5}O_2$ as a catalyst. It was found that the methane conversion was improved. Moreover, sweep gas also helps for improving the conversion.